

Article

## Synthesis, Characterization and Texture Observations of Calamitic Liquid Crystalline Compounds

Maher A. Qaddoura<sup>1</sup> and Kevin D. Belfield<sup>1,2,\*</sup>

<sup>1</sup> Department of Chemistry; University of Central Florida, P.O. Box 162366, Orlando, FL 32816-2366, USA; E-Mail: mqaddour@mail.ucf.edu (M.A.Q.)

<sup>2</sup> CREOL, The College of Optics and Photonics, University of Central Florida, P.O. Box 162366, Orlando, FL 32816-2366, USA

\* Author to whom correspondence should be addressed; E-Mail: belfield@mail.ucf.edu.

Received: 1 September 2009; in revised form: 1 October 2009 / Accepted: 19 October 2009 /

Published: 4 November 2009

---

**Abstract:** Several divinyllic mesogenic monomers were synthesized based on coupling the monomer 4-(4-pentenyl)benzoic acid with chlorohydroquinone, 2,5-dihydroxyacetophenone, methylhydroquinone or 2-methoxyhydroquinone. This resulted in novel mesogens of phenylene esters with different lateral substituent groups. The effect of the lateral substituent group on the thermotropic phase behavior for these liquid crystalline compounds was investigated using DSC and optical polarized microscopy. All the mesogens proved to have a wide nematic liquid crystalline range. Only the phenylene ester, which has a methoxy lateral substituent, exhibited both nematic and smectic phases. Structural confirmation of all new derivatives was accomplished by <sup>1</sup>H- and <sup>13</sup>C-NMR spectroscopic analysis, along with CH elemental analysis.

**Keywords:** liquid crystalline texture; nematic phase; smectic phase

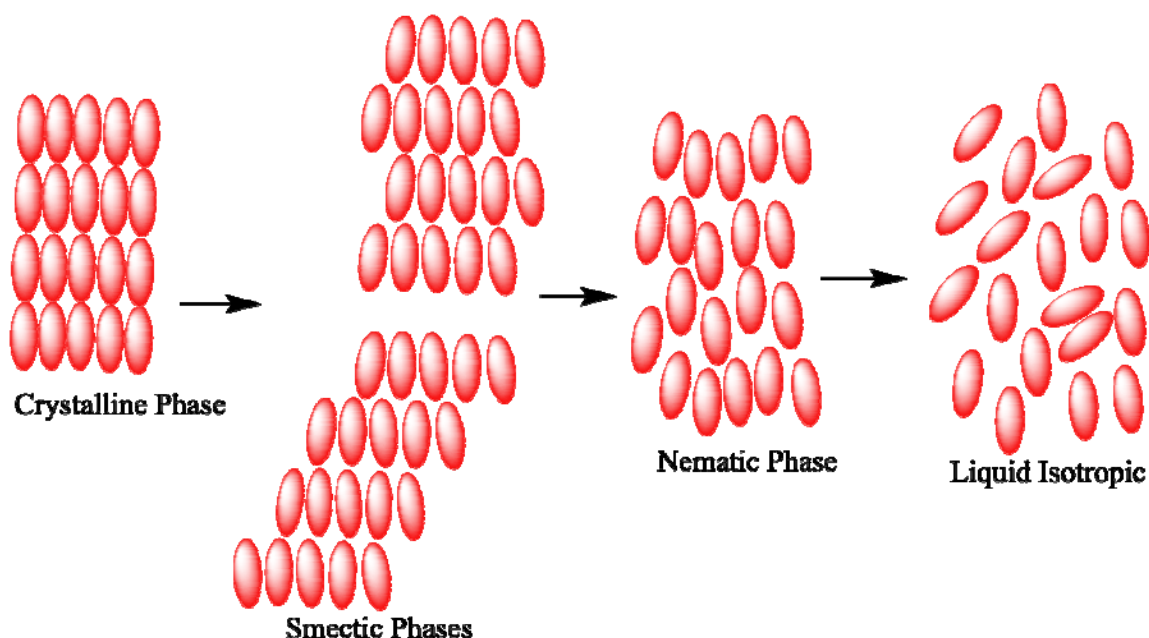
---

### 1. Introduction

Liquid crystalline behavior has been observed mainly in two types of molecules: linear or rod-like molecules that form calamitic phases and disc-like molecules that form discotic phases. The structure of liquid crystalline phases is characterized by the arrangement of the molecules, the conformation of the molecules, and the intermolecular interactions. The transition between the various liquid crystal

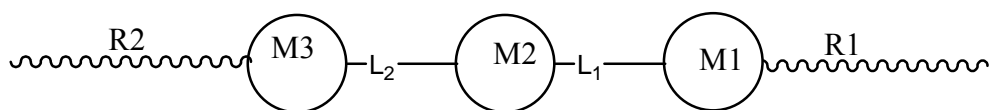
mesophases from crystalline to smectic to nematic occurs at defined temperatures which can be detected using differential scanning calorimetry, while the nature and texture of the mesophase is normally investigated using polarized optical microscopy. The scenario involving phase transitions requires, as the first step, the breakdown of the molecular packing order under influence of an external heating source causing oscillation, or rapid rotation about the long axis of the molecule to give a ‘smectic-like’ crystal phase. Next, the long-range positional order is lost resulting in a smectic liquid crystal mesophase. Next, the local packing order is destroyed, but the orientational order still remains with the molecules reorganizing so that their long axes lie in the same direction producing the nematic phase. Finally, all order is lost forming an isotropic liquid[1]. The description of this melting process for rod-like molecules is shown schematically in Figure 1.

**Figure 1.** Phase transition between crystals, smectic, nematic, and isotropic liquid phases for a calamitic material as function of temperature.



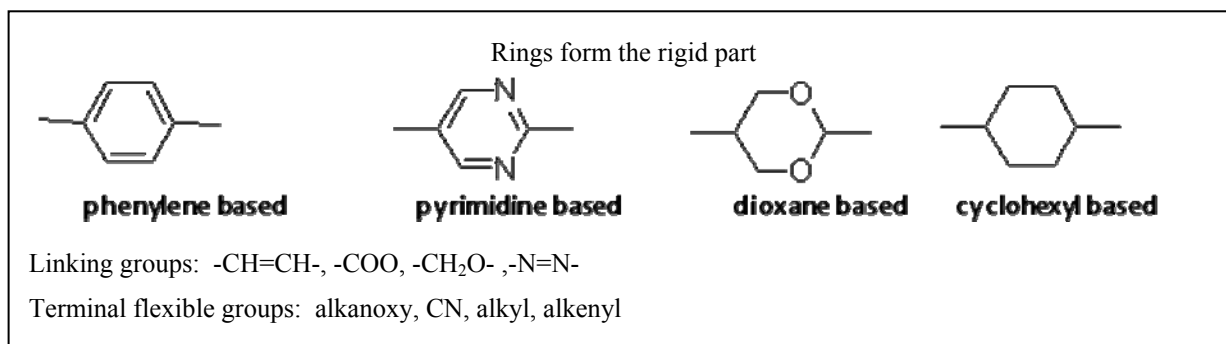
Calamitic liquid crystals are characterized by their elongated, rod-like shape, and composed of three main structural elements: rigid ring systems, connective linkage groups, and flexible terminal groups. A general structure is given in Figure 2.

**Figure 2.** Model represents typical feature of calamitic liquid crystals, R1 & R2 are terminal groups, M1, M2 & M3 are ring systems, and L1 & L2 are linking groups.



Here, R1 and R2 are terminal groups, M1, M2, and M3 are ring systems and usually two to four of these units are present; they could be identical or different groups, and, finally, L represents linking groups. The most common of these, along with typical rings and linking groups, are listed in Figure 3 [2]. A wide range of lateral substituents (*e.g.*, F, Cl, CN, NO<sub>2</sub>, CH<sub>3</sub>, CF<sub>3</sub>) have been incorporated into many liquid crystal structures; a lateral substituent is one that is attached off the linear axis of the molecule, usually on the side of an aromatic core or even alicyclic moieties. The presence of the lateral substituents leads to disruption of molecular packing and, therefore, reduces liquid crystalline phase stability. This disruption of the molecular packing is particularly advantageous for the mesomorphic and physical properties required for specific applications. In general, the depression of the clearing point expressed as  $T_{N-1}$  by a lateral substituent is directly proportional to the substituent size, irrespective of its polarity [2].

**Figure 3.** Examples of typical groups which represent the main constituents of calamitic liquid crystalline molecules.



Polarized light microscopy is commonly used to identify the texture of liquid crystalline mesophases. The textures are pictures that are observed microscopically under polarized light and characterized by defects of the phase structure that are generated by the distortion of the phase structure by the surrounding glass slides and coverslips (surface phenomena). Therefore, several different textures can be observed for a given structure depending on the particular conditions of sample preparation [3]. For example, an isotropic liquid will be dark under crossed polars, while birefringent liquid crystals exhibit interference colors.

A thin sample of the nematic phase, when viewed under polarizing microscopy, is often seen optically extinct, and appears dark. However, there may be small areas of a birefringent texture with dark (optically extinct) thread-like defects if the sample is thick. Displacement of the coverslip (shearing) induces homogenous (planar) alignment, producing a temporary birefringent flash. On heating the sample, homogeneous alignment is often induced close to the clearing point. It is at this point that the phase appears most colorful (schlieren texture) and a thin sample looks particularly sharp and is readily imaged [2,4].

When cooling an isotropic liquid, birefringent droplets appear against a dark background as the nematic phase is generated. In thick samples, these droplets coalesce to give a schlieren texture that may contain the thread-like defects. On cooling, the nematic phase appears from the isotropic liquid and so the texture that results is called a natural texture.

Calamitic liquid crystals based on p-alkoxy benzoic acid were investigated earlier for their liquid crystalline properties [5,6], and recently gained increased interest for the design of many liquid crystalline compounds. Demus *et al.* were among the first researchers to use calamitic liquid crystals for practical applications in the LCD industry [7-10]. However, the terminal end of the compounds were unfunctionalized linear aliphatic chains. On the other hand, alkenyloxy benzoate monomers are a functionalized version of alkoxy benzoate, a construct that also gained special attention in the design of functionalized liquid crystalline materials [11-15].

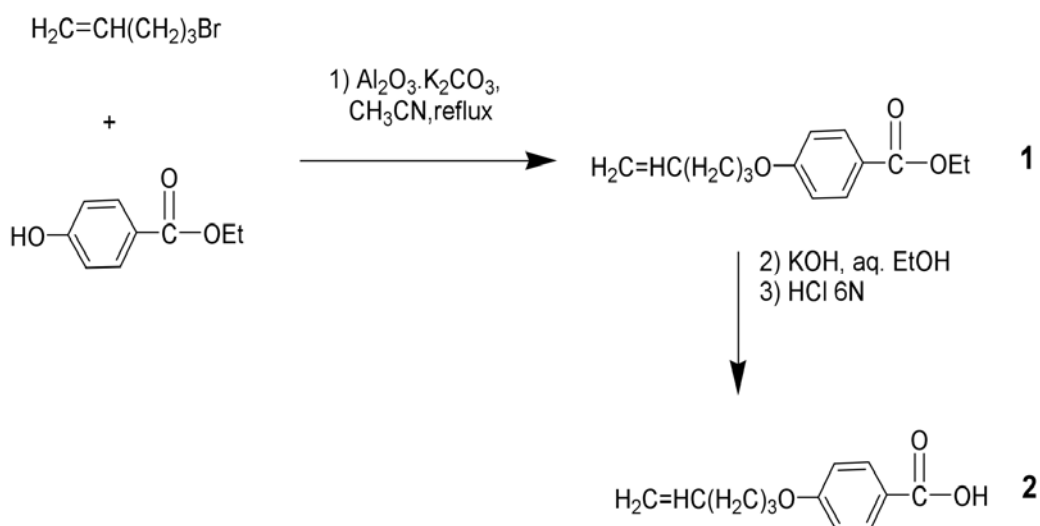
Reported herein are divinyllic calamitic liquid crystals that are based on functionalized alkenyloxy benzoates coupled with dihydroquinone derivatives. These represent attractive functionalized compounds for use as precursors to design more advanced materials, *e.g.*, when crosslinked with siloxanes. This type of versatile crosslinking may result in unique liquid crystalline polymers and elastomers with potential applications in the field of artificial muscles [16], separation membranes, optical materials, bifocal contact lenses [17-19], holography [20], drug delivery [21], and electro-optics [22]. We have designed and synthesized a series of functionalized divinyllic calamitic liquid crystals with different lateral substituents. These materials have been fully characterized, including their thermal behavior and texture observations.

## 2. Results and Discussion

### 2.1. Synthesis of 4-(4-Pentenyl)oxybenzoic Acid

The synthesis of alkenyloxycarboxylic acid **2** is shown in Scheme 1; ethyl 4-hydroxybenzoate was etherified with 5-bromo-1-pentene in the presence of a catalyst system comprised of potassium carbonate supported on alumina. This system gave a high yield of product **1** with a minimum reaction time of 4 h. This is significant since many researchers have used different catalyst systems, such as  $K_2CO_3$  in acetone or KOH in ethanol, producing lower yields and requiring longer reaction times (typically 12-48 h) [23-27].  $^1H$  and  $^{13}C$  spectra were consistent with the proposed structure for **1**.

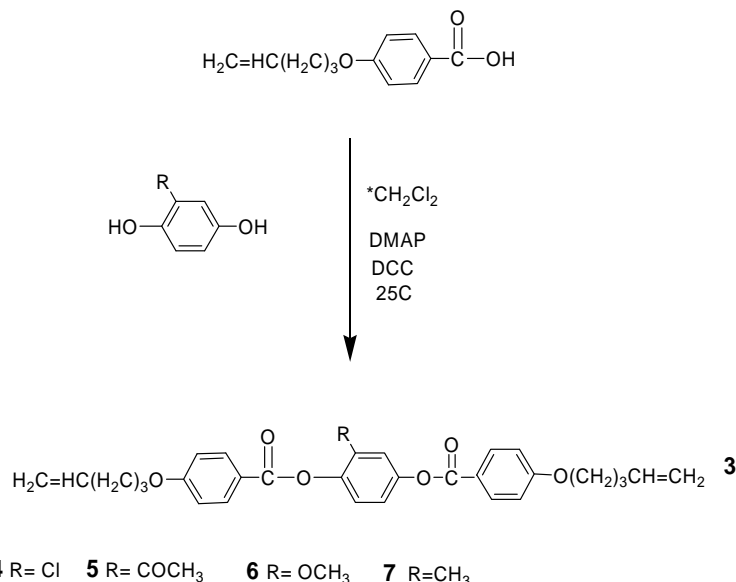
**Scheme 1.** Synthesis of 4-(4-pentenyl)oxybenzoic acid).



## 2.2. Synthesis and Thermotropic Behavior of Benzoate Mesogenic Compounds

Four mesogenic structures, having the general structure **3** but with different lateral substituents, have been synthesized as shown in Scheme 2.

**Scheme 2.** Synthesis of the calamitic liquid crystalline structures.

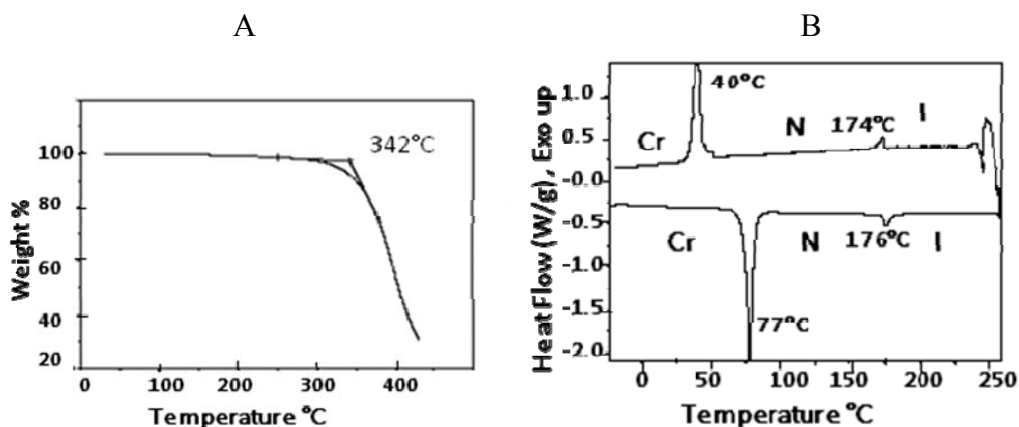


\* Methylene chloride was mixed with 10% acetone for the reaction of 2-methoxyhydroquinone with the above monomer.

### 2.2.1. Benzoic Acid, 4-(4-Pentenyl)-, 2-Chloro-1,4-phenylene Ester (**4**)

As shown in Scheme 2, mesogen **4** was synthesized by esterification of 2-chlorohydroquinone with 4-(4-pentenyl)benzoic acid (**2**), in the presence of DCC. <sup>1</sup>H- and <sup>13</sup>C-NMR spectra were consistent with the structure proposed for **4**. CH analysis results were within acceptable limits. TGA showed that the mesogen started to decompose at 342 °C (Figure 4 A). Figure 4 B shows DSC thermograms of compound **4**.

**Figure 4.** Thermogravimetric analysis and DSC graph of benzoic acid, 4-(4-pentenyl)-, 2-chloro-1,4-phenylene ester (**4**).



It displayed a nematic phase on both heating and cooling. The thermotropic behavior and the enthalpy values are given in Table 1. One can clearly see that higher energy is required for the transition from the crystalline to the nematic phase ( $7.13 \text{ kcal mol}^{-1}$ ) while less energy is needed for the nematic to crystalline phase transition ( $0.47 \text{ kcal mol}^{-1}$ ). This is due to the fact that larger energy is needed to disrupt both the positional and the orientational order of the crystalline phase; while less energy is needed to disrupt the orientational order of the nematic phase.

**Table 1.** Phase transition temperatures and enthalpy changes of compound 4.

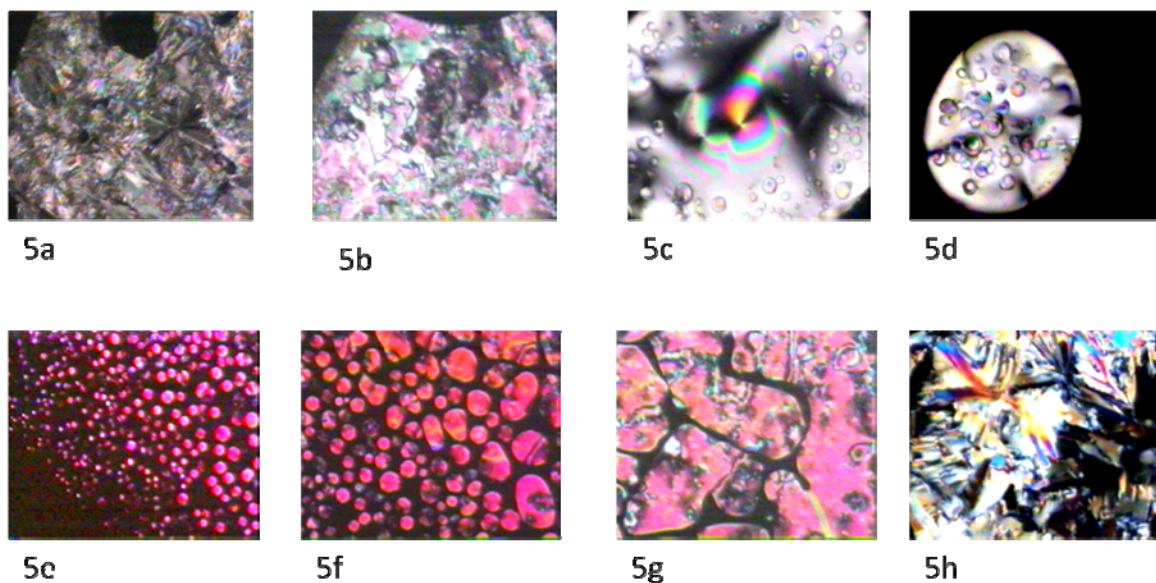
<i>Heating</i>		
Phase Transition	Temperature °C	$\Delta H \text{ kJmol}^{-1}$
Cr-N	77.3	29.8
N-I	176	1.95

<i>Cooling</i>		
Phase Transition	Temperature °C	$\Delta H \text{ kJmol}^{-1}$
I-N	174	1.95
N-Cr	40.0	25.2

I: isotropic, N:nematic, Cr: crystalline

**Figure 5.** (5a) Crystalline texture of the mesogen; crossed polarizers,  $25 \text{ }^\circ\text{C}$ ,  $\times 150$ . (5b) Nematic texture; crossed polarizers,  $77.3 \text{ }^\circ\text{C}$ ,  $\times 150$ . (5c).Nematic–Isotropic transition; crossed polarizers. $176 \text{ }^\circ\text{C}$ ,  $\times 150$ . (5d). Nematic –Isotropic Transition. The black domain is the isotropic phase with no optical activity; crossed polarizers, $176 \text{ }^\circ\text{C}$ ,  $\times 150$ . (5e) Nematic droplets appear from the isotropic phase; crossed polarizers,  $174 \text{ }^\circ\text{C}$ ,  $\times 150$ . (5f) Nematic droplets starts to coalesce to form the nematic texture; crossed polarizers,  $174 \text{ }^\circ\text{C}$ ,  $\times 150$ . (5g) Nematic domain becomes more apparent and threadlike texture is appearing; crossed polarizers,  $174 \text{ }^\circ\text{C}$ ,  $\times 150$ . (5h) Crystalline texture; crossed polarizers, below  $40 \text{ }^\circ\text{C}$ ,  $\times 150$ .



Mesophase identification was achieved by optical polarized light microscopic observations. Figure 5 illustrates crystalline phases of mesogen **4**, with magnification of 150x under crossed polarizers. By bringing the temperature up to 77 °C, a crystalline to nematic transition was observed (Figure 5b). On further heating up to 174 °C, the nematic phase lost its birefringence and was transformed to an isotropic phase (Figures 5c and 5d). By cooling the isotropic phase at 10 °C/min, nematic droplets began to appear and coalesce (Figures 5e and 5f), forming a nematic texture (Figure 5g). The texture color change is due to the sensitivity of the birefringent nematic mesophase to temperature. Finally, when the temperature was reduced to 40 °C, a crystalline texture formed (Figure 5h).

### 2.2.2. Benzoic Acid, 4-(4-Pentyloxy)-, 2-Acetyl-1,4-phenylene Ester (**5**)

Mesogen **5** was synthesized according to Scheme 2 by esterification of 2-hydroxyacetophenone with **2** in presence of DCC. A 1:10 mixture (by volume) of anhydrous acetone with methylene chloride was used in the reaction to insure complete miscibility of 2-hydroxyacetophenone. <sup>1</sup>H- and <sup>13</sup>C-NMR spectra were consistent with the structure suggested for **5**. CH analysis results were within acceptable limits. The thermogravimetric analysis showed that the mesogen began decomposing at 307 °C, as can be seen from Figure 6a. Figure 6B shows DSC thermograms of compound **5**. One can clearly see the presence of a nematic phase on both heating and cooling. The thermotropic behavior and the enthalpy values are presented in Table 2.

**Figure 6.** (6A) Thermogravimetric analysis of benzoic acid, 4-(4-pentyloxy)-, 2-acetyl-1,4-phenylene ester (**5**). (6B) DSC thermograms for benzoic acid, 4-(4-pentyloxy)-, 2-acetyl-1,4-phenylene ester (**5**).

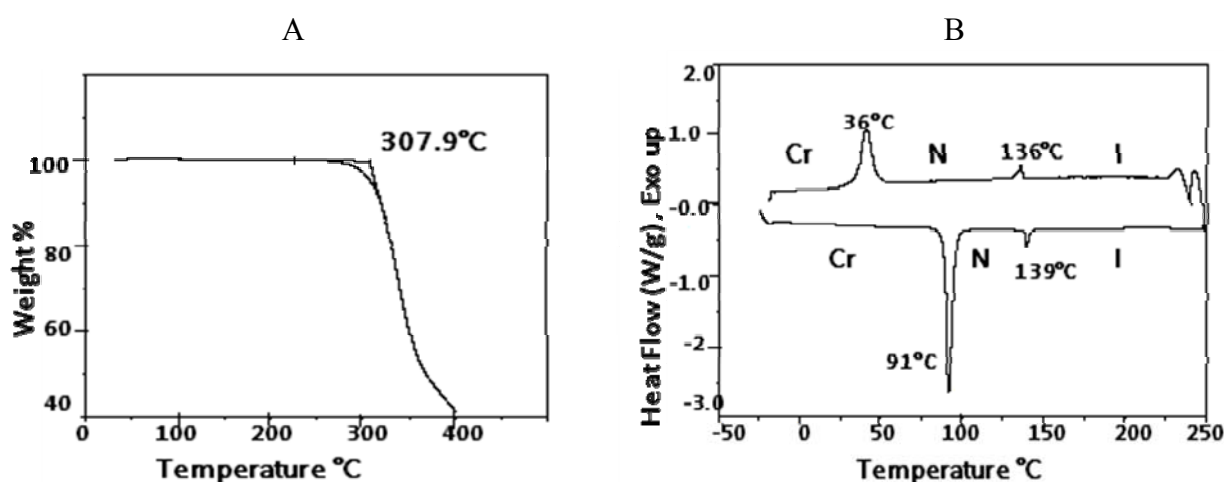


**Table 2.** Phase transition temperatures and enthalpy changes of compound **5**.

<i>Heating</i>		
Phase Transition	Temperature °C	$\Delta H$ kJmol <sup>-1</sup>
Cr-N	91.0	35.4
N-I	139	2.30



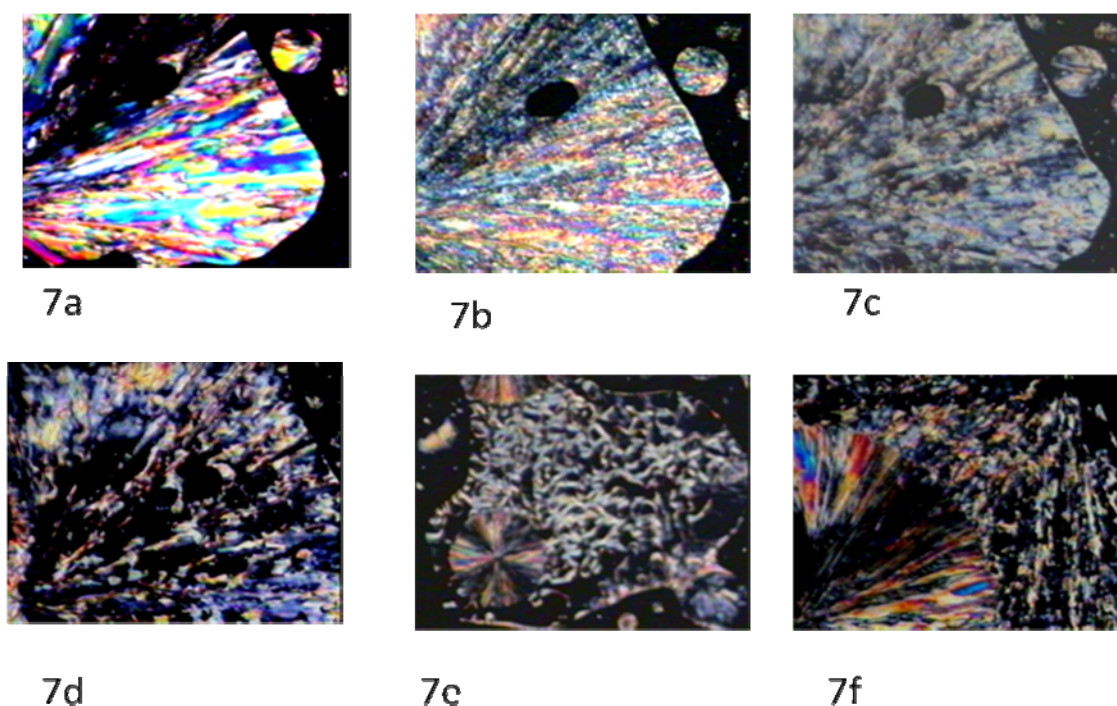
Table 2. Cont.

<i>Cooling.</i>		
Phase Transition	Temperature °C	$\Delta H \text{ kJmol}^{-1}$
I-N	136	-2.36
N-Cr	36.0	-23.0

I: isotropic, N:nematic, Cr: crystalline.

The mesophase identification was achieved by optical polarized light microscopic observations. Figures 7 shows crystalline phases for mesogen **5**. Upon heating, a phase transition occurred and a nematic texture was observed (Figures 7a and 7b). When the temperature was brought up to 139 °C, an isotropic phase was observed (Figure 7c). Upon cooling of the isotropic phase, a nematic texture was observed, followed by crystalline phase appearance at 36 °C (Figures 7d, 7e, and 7f).

**Figure 7.** (7a) Initial crystalline texture of the mesogen; cross polarizers, 25 °C,  $\times 150$ . (7b) Crystalline-Nematic transition; crossed polarizers, 90.5 °C,  $\times 150$ . (7c) Nematic phase; 91 °C,  $\times 150$ . (7d) Nematic-Isotropic transition upon heating. The black domain represents the isotropic phase; crossed polarizers, 139 °C,  $\times 150$ . (7e) Nematic-Crystalline transition upon cooling; crossed polarizers 36 °C,  $\times 150$ . (7f) Nematic-Crystalline transition; crossed polarizers 36 °C,  $\times 150$ .



### 2.2.3. Benzoic Acid, 4-(4-pentenloxy)-, 2-Methoxy-1,4-phenylene Ester (**6**): Synthesis

As shown in Scheme 2, mesogen **6** was synthesized by esterification of 2-methoxyhydroquinone with **2** in the presence of DCC.  $^1\text{H}$ - and  $^{13}\text{C}$ -NMR spectra were consistent with the structure for **6**, and CH analysis results were within acceptable limits.



TGA data indicated that compound **6** began to decompose at 342 °C (Figure 8a). Figure 8b represents DSC thermograms of compound **6**. Smectic and nematic phases were observed on both heating and cooling. The thermotropic behavior and the enthalpy values are listed in Table 3.

Mesophase identification of compound **6** was achieved by optical light polarized microscopic observations. When the temperature was raised to 97 °C, a change was observed under the microscope (Figure 9a). Figure 9b shows a smectic phase (likely smectic A) with focal domains and broken fans texture, a characteristic features of smectic phases. A transition from the smectic to nematic phase was observed at 111 °C and a nematic to isotropic transition was observed at 142 °C. Upon cooling the isotropic phase, nematic droplets appeared from the isotropic phase; these droplets coalesce to form a nematic phase texture, which results in a point of defects and two and four brushes; see Figures 9c. On further cooling to 57 °C, the smectic phase has appeared for a very short period of time, often being undetected by DSC or under the microscope (see Figure 9d). Finally, at 36 °C, a crystalline phase was observed.

**Figure 8.** (8a) Thermogravimetric analysis of benzoic acid, 4-(4-pentenylloxy)-, 2-methoxy-1,4-phenylene ester (**6**). (8b) DSC thermograms for benzoic acid, 4-(4-pentenylloxy)-, 2-methoxy-1,4-phenylene ester (**6**).

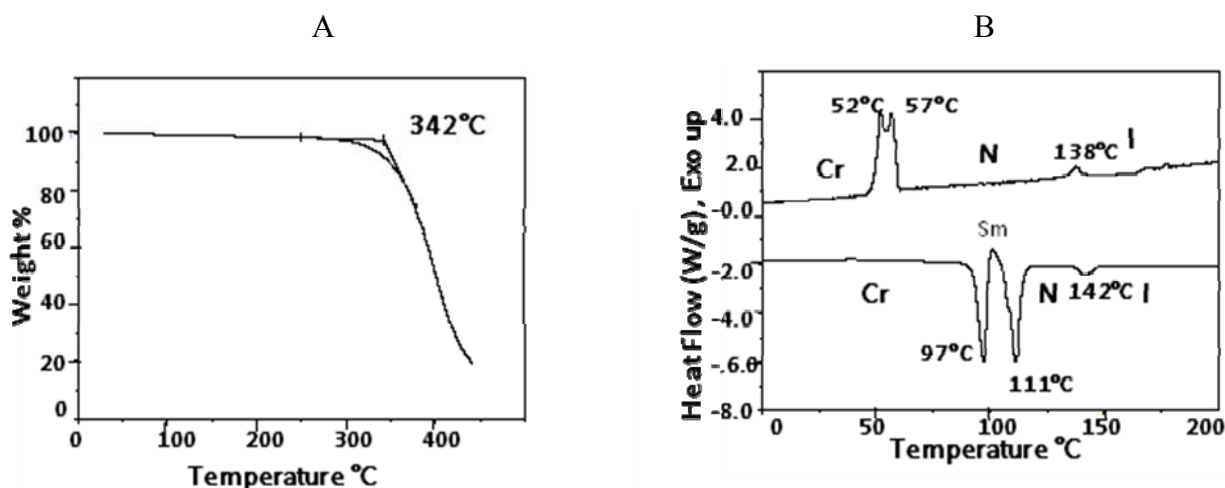
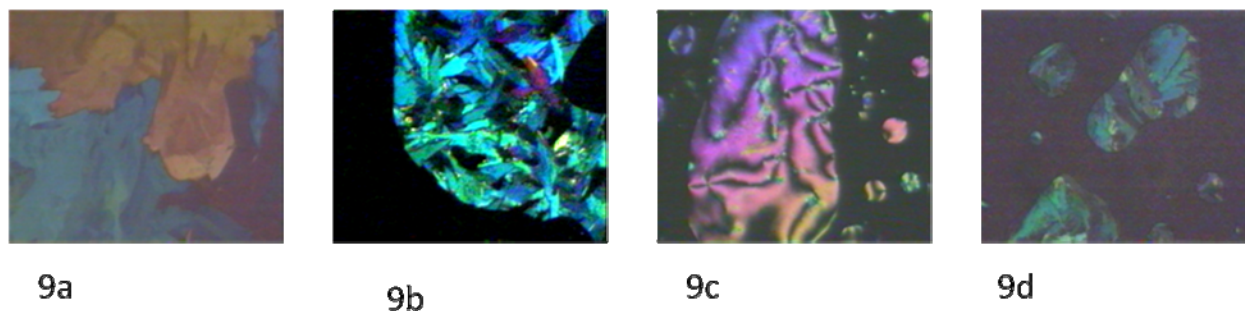


**Table 3.** Phase transition temperatures and enthalpy changes compound **6**.

<i>Heating</i>		
Phase Transition	Temperature °C	$\Delta H$ kJmol <sup>-1</sup>
Cr-Sm	97.0	5.50
Sm-N	111	7.45
N-I	142	0.65
<i>Cooling</i>		
Phase Transition	Temperature °C	$\Delta H$ kJmol <sup>-1</sup>
I-N	138	-0.80
N-Sm	57	Coincided peaks
		Total= -8.1
Sm-Cr	52	Coincided peaks

I: isotropic, N:nematic, Sm: smectic, Cr: crystalline.

**Figure 9.** (9a) Crystalline-Smectic phase transition state; crossed polarizers, 97 °C,  $\times 150$ . (9b) Smectic phase (smectic A) with broken fan-shape texture; crossed polarizers, 97 °C,  $\times 150$ . (9c) Nematic schlieren texture with point singularities; crossed polarizers, below 138 °C,  $\times 150$ . (9d) Smectic phase upon cooling exhibited broken fans; crossed polarizers, 57 °C,  $\times 150$ .



#### 2.2.4. Benzoic Acid, 4-(4-Pentenloxy)-, 2-Methyl-1,4-phenylene Ester (7)

As shown in Scheme 2, mesogen **7** was synthesized by esterification of 2-methylhydroquinone with **2** in the presence of DCC.  $^1\text{H}$ - and  $^{13}\text{C}$ -NMR spectra were consistent with the structure for **7**. The  $^1\text{H}$ -NMR spectrum was identical to that reported in the literature [26]. TGA indicated that mesogen **7** started to decompose at 335 °C, as seen from Figure 10a. Figure 10b shows the DSC thermograms of compound **7**, revealing nematic phases on both heating and cooling. The thermotropic behavior and the enthalpy values are listed in Table 4.

**Figure 10.** (10A) Thermogravimetric analysis of benzoic acid, 4-(4-pentenloxy)-, 2-methyl-1,4-phenylene ester (**7**). (10B) DSC thermograms for benzoic acid, 4-(4-pentenloxy)-, 2-methyl-1,4-phenylene ester (**7**).

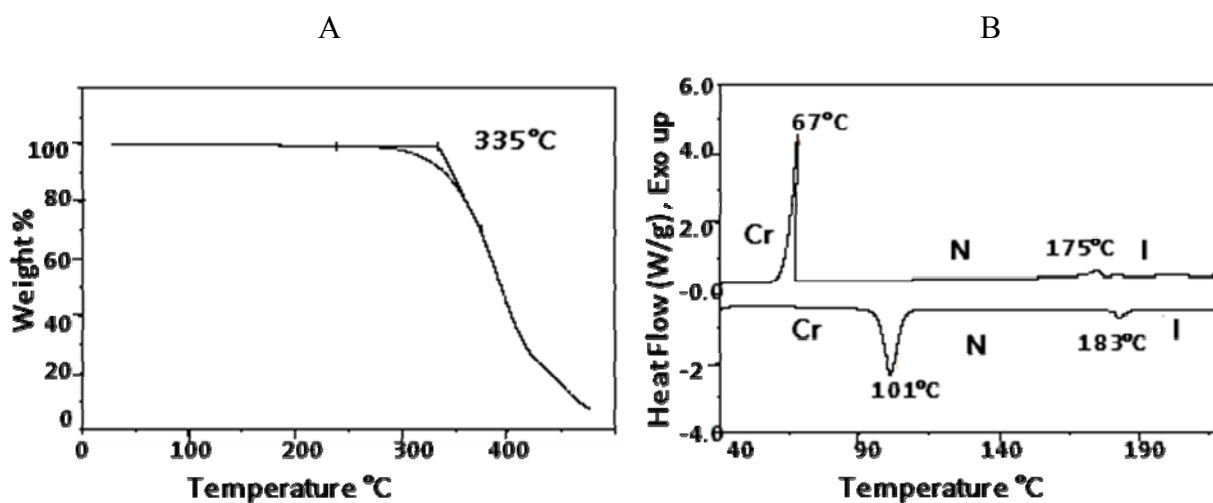


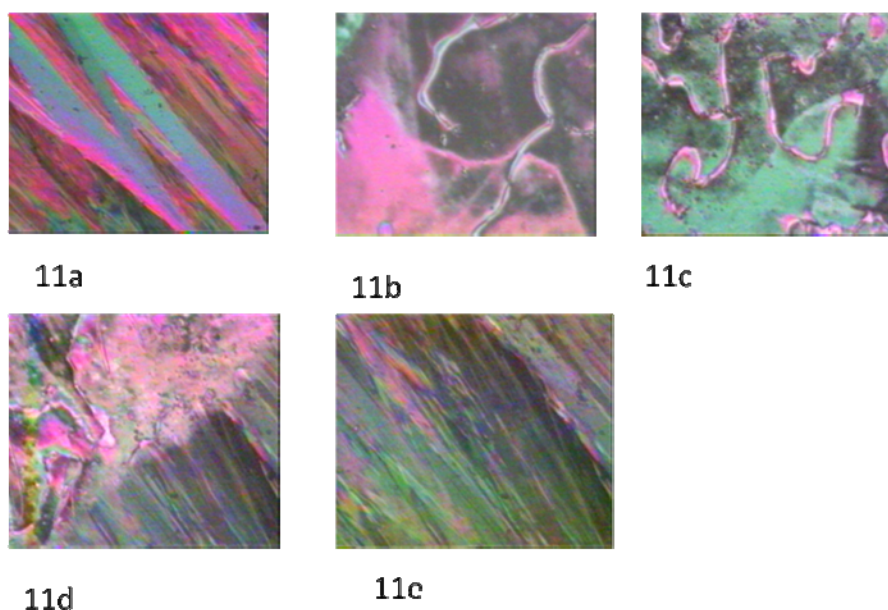
**Table 4.** Phase transition temperatures and enthalpy changes for compound 7.

<i>Heating</i>		
Phase Transition	Temperature °C	$\Delta H$ kJmol <sup>-1</sup>
Cr-N	101	35.0
N-I	183	2.5
<i>Cooling</i>		
Phase Transition	Temperature °C	$\Delta H$ kJmol <sup>-1</sup>
I-N	175	-2.28
N-Cr	67	-31.1

I: isotropic, N:nematic, Cr: crystalline.

Texture identification for mesogen 7 has been achieved by optical polarized light microscopic observations. Figure 11a presents the crystalline phase of the mesogen. Upon heating up to 101 °C, a phase transition was observed, exhibiting thread-like nematic texture (Figure 11b). On further heating to 131 °C, the nematic to isotropic phase transition occurred. Upon cooling, nematic droplets emerged and coalesced to form a nematic texture (Figure 11c). The nematic texture was characterized by its thread-like texture and line defects. On further cooling to 67 °C, the crystalline phase began replacing the nematic phase (Figures 11d and 11e).

**Figure 11.** (11a) Crystalline texture of the mesogen; crossed polarizers, 25 °C, ×150. (11b) Nematic thread-like texture; crossed polarizers, 101 °C, ×150. (11c) Nematic thread-like texture; crossed polarizers, below 175 °C, ×150. (11d) Nematic-Crystalline phase transition; crossed polarizers, 67 °C, ×150. (11e) Crystalline phase; crossed polarizers, below 67 °C, ×150.



### 2.3. The Effect of Lateral Substituent Size on the Clearing Point.

It was found that the nematic-isotropic ( $T_{N-I}$ ) transition temperatures decreased by increasing the lateral substituent size (Figure 12) in the following order:



**Figure 12.** Lateral substitution in the mesogen.

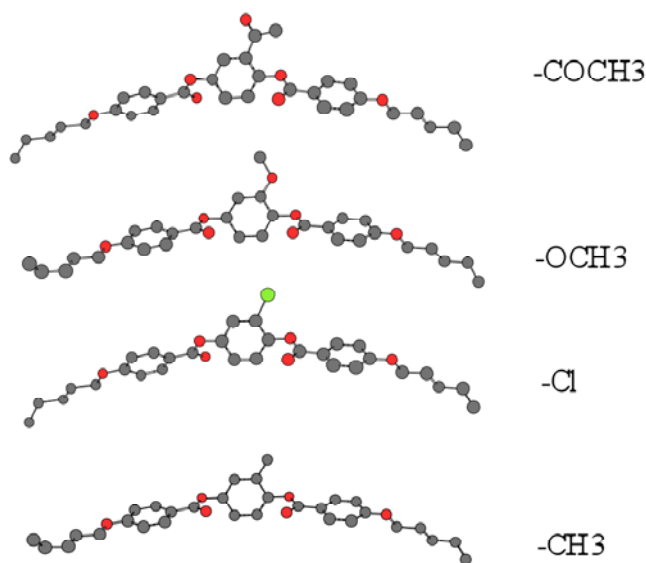


Figure 12 shows the size of lateral substituents in the mesogens, as calculated by MM2 energy minimization computational analysis using the Cambridge Scientific Chem 3D program. As anticipated, the more bulky the substituent, the lower the packing density of the molecules, and the weaker the Van der Waals intermolecular forces of attraction. This results in decreased clearing temperatures with increased size of the lateral substituents. This molecular design strategy provides an excellent method to modulate the clearing temperature of this class of liquid crystalline materials.

## 3. Experimental Section

### 3.1. Materials

5-Bromo-1-pentene (97%), 2,5-dihydroxyacetophenone (97%), 2-methoxyhydroquinone (97%), potassium carbonate (99+%) were used as received from Lancaster. 4-(Dimethylamino)pyridine (DMAP, 99%), 1,3-dicyclohexylcarbodiimide (DCC, 99%), methylhydroquinone (99%), ethyl hydroxybenzoate (99%) were used as received from Aldrich. Chlorohydroquinone (94+%) was used as received from Alfa Aesar. MN-Aluminum Oxide, neutral (manufactured by Machery Nagel & Co) was used as received. Commercial methylene chloride was distilled from lithium aluminum hydride and stored over molecular sieves in a sealed container. THF was dried by distillation over sodium, and stored over molecular sieves in a sealed container. HPLC grade acetonitrile was dried using molecular

sieves and stored in a sealed container. All other reagents and solvents were commercially available, unless noted otherwise.

### 3.2. Instrumentation

Thermogravimetric analysis (TGA) was performed using a TGA 2050 thermogravimetric analyzer (TA Instruments) at a heating rate of 20 °C/min. The thermotropic behavior of all compounds was determined by a combination of differential scanning calorimetry (DSC) and polarized optical microscopy. A TA Instruments 2920 differential scanning calorimeter (DSC) was used to determine the thermal transitions that were read as the maximum or minimum of the endothermic or exothermic peaks, respectively. All heating and cooling rates were 10 °C/min. Unless stated otherwise, thermal transitions were read from reproducible second or later heating scans and first or later cooling scans, respectively. An Olympus BH-2 polarized optical microscope (magnification  $\times 150$ ), equipped with a Mettler FP52 hot stage, was used to detect and image phase transitions. Images were captured using a video camera and frame grabber software. Thin samples were prepared by melting a minimum amount of compound between a clean glass slide and a cover slip.  $^1\text{H}$ - and  $^{13}\text{C}$ -NMR analyses were performed in  $\text{CDCl}_3$  (referenced to TMS at  $\delta$  0.0 ppm) on a Varian Gemini spectrometer (300 MHz for  $^1\text{H}$  and 75 MHz for  $^{13}\text{C}$ ).

### 3.3. Synthesis

#### 3.3.1. Preparation of the $\text{K}_2\text{CO}_3 \cdot \text{Al}_2\text{O}_3$ Catalyst

Potassium carbonate (103 g, 0.74 mmol) was mixed with neutral aluminum oxide (150 g, 1.47 mmol) in distilled water (300 mL). The mixture was stirred and heated to 50 °C for 1 h. The water was evaporated, and the resulting catalyst was activated overnight in the oven at 120 °C.

#### 3.3.2. Ethyl 4-(4-Pentenyl)benzoate [27]

A solution of 5-bromo-1-pentene (12.6 g, 85 mmol) was added dropwise to a refluxing solution of ethyl 4-hydroxybenzoate (15 g, 90 mmol) and alumina-supported potassium carbonate (the catalyst). After 5 h of reflux, the reaction mixture was poured into water and extracted three times with methylene chloride (400 mL total). The organic layer was filtered to remove any traces of the catalyst. The solvent was removed on a rotary evaporator *in vacuo* to yield 19.2 g (97%) of ethyl 4-(4-pentenyl) benzoate as a slightly yellowish oil.  $^1\text{H}$ -NMR ( $\delta$  ppm TMS,  $\text{CDCl}_3$ ): 1.38 (t,  $\text{CO}_2\text{CH}_2\text{CH}_3$ ), 1.90 (m,  $\text{CH}_2\text{CH}_2\text{O}$ ), 2.25 (q,  $\text{CH}_2\text{CH}=\text{CH}_2$ ), 4.02 (t,  $\text{OCH}_2$ ), 4.34 (q,  $\text{CO}_2\text{CH}_2$ ), 5.05 (m,  $=\text{CH}_2$ ), 5.85 (m,  $=\text{CH}$ ), 6.90 (d, 2 aromatic H ortho to OR), 7.98 (d, 2 aromatic H ortho to  $\text{CO}_2\text{R}'$ );  $^{13}\text{C}$ -NMR ( $\delta$  ppm TMS,  $\text{CDCl}_3$ ):  $\delta$  14.7, 28.6, 30.3, 60.8, 67.5, 114.1, 115.5, 122.9, 131.6, 137.7, 162.9, 166.7.

### 3.3.3. 4-(4-Pentenyl)oxybenzoic Acid (**1**) [27]

Ethyl 4-(4-pentenyl)oxybenzoate (19.2 g, 82 mmol) and potassium hydroxide (15 g, 0.27 mol), dissolved in ethanol (50 mL) and water (100 mL), were refluxed for 6 h. After being cooled to room temperature, the solution was acidified to pH 2 with concentrated HCl. The resulting precipitate was collected and recrystallized from ethanol, affording 15.2 g (90%) of 4-(4-pentenyl)oxybenzoic acid (**1**) as white shiny crystals.  $^1\text{H-NMR}$  ( $\delta$  ppm TMS,  $\text{CDCl}_3$ ): 1.92 (m,  $\text{CH}_2\text{CH}_2\text{O}$ ), 2.24 (q,  $\text{CH}_2\text{CH}=\text{CH}_2$ ), 4.04 (t,  $\text{OCH}_2$ ), 5.05 (m,  $=\text{CH}_2$ ), 5.86 (m,  $\text{CH}=\text{CH}_2$ ), 6.93 (d, 2 aromatic H ortho to OR), 8.05 (d, 2 aromatic H ortho to  $\text{CO}_2\text{H}$ );  $^{13}\text{C-NMR}$  ( $\delta$  ppm TMS,  $\text{CDCl}_3$ ):  $\delta$  28.2, 30.0, 67.3, 114.0, 115.2, 121.3, 132.1, 137.3, 163.3, 171.8.

### 3.3.4. Benzoic Acid, 4-(4-Pentenyl)oxy-, 2-Chloro-1,4-phenylene Ester (**4**)

4-(4-Pentenyl)oxybenzoic acid (**1**) (1.04 g, 5.1 mmol), chlorohydroquinone (0.4 g, 2.8 mmol), DMAP (0.05 g, 0.4 mmol), and DCC (1.04 g, 5.1 mmol) in dry  $\text{CH}_2\text{Cl}_2$  (15 mL) were stirred at room temperature for 48 h. The reaction mixture was then extracted with water and methylene chloride. The precipitate of the dicyclohexylurea by-product was filtered off and discarded. The solvent was removed using a rotary evaporator. The resulting solid was recrystallized from ethanol, yielding 1.2 g (70%) of benzoic acid, 4-(4-pentenyl)oxy-, 2-chloro-1,4-phenylene ester (**4**) as white crystals.  $^1\text{H-NMR}$  ( $\delta$  ppm TMS,  $\text{CDCl}_3$ ): 1.95 (m,  $\text{CH}_2\text{CH}_2\text{O}$ , 4 H), 2.26 (m,  $\text{CH}_2\text{CH}=\text{CH}_2$ , 4 H), 4.06 (t,  $\text{OCH}_2$ , 4 H), 5.05 (m,  $=\text{CH}_2$ , 4 H), 5.85 (m,  $=\text{CH}$ , 2 H), 6.97 (dd, 4 aromatic H ortho to OR), 7.17 (m, 3 aromatic H of central ring), 8.13 (dd, 4 aromatic H ortho to  $\text{CO}_2\text{Ar}$ );  $^{13}\text{C-NMR}$  ( $\delta$  ppm TMS,  $\text{CDCl}_3$ ):  $\delta$  28.6, 30.4, 67.778, 114.6, 115.7, 121.4, 124.0, 124.4, 127.2, 132.7, 137.7, 144.3, 148.2, 163.7, 164.1; Anal. Calcd. for  $\text{C}_{30}\text{H}_{29}\text{ClO}_6$ : C, 69.16; H, 5.61; Cl, 6.80, found: C, 69.00; H, 5.66; Cl, 6.80.

### 3.3.5. Benzoic Acid, 4-(4-Pentenyl)oxy-, 2-Acetyl-1,4-phenylene Ester (**5**)

4-(4-Pentenyl)oxybenzoic acid (**1**, 1.04 g, 5.1 mmol), 2,5-dihydroxyacetophenone (0.4 g, 2.6 mmol), DMAP (0.05 g, 0.4 mmol), DCC (1.04 g, 5.1 mmol), dry  $\text{CH}_2\text{Cl}_2$  (15 mL), and dry acetone (2 mL), were stirred at room temperature for 48 h. Extraction of the product was carried out with water and methylene chloride. The precipitate of dicyclohexylurea by-product was filtered off and discarded. The solvent was removed using a rotary evaporator. The resulting solid was recrystallized from ethanol, providing 0.69 g (50%) of benzoic acid, 4-(4-pentenyl)oxy-, 2-acetyl-1,4-phenylene ester (**5**) as white crystals.  $^1\text{H-NMR}$  ( $\delta$  ppm TMS,  $\text{CDCl}_3$ ): 1.94 (m,  $\text{CH}_2\text{CH}_2\text{O}$ , 4 H), 2.27 (m,  $\text{CH}_2\text{CH}=\text{CH}_2$ , 4 H), 2.54 (s,  $\text{O}=\text{CCH}_3$ ), 4.06 (t,  $\text{OCH}_2$ , 4 H), 5.05 (m,  $=\text{CH}_2$ , 4 H), 5.85 (m,  $=\text{CH}$ , 2 H), 6.97 (dd, 4 aromatic H ortho to OR), 7.46 (m, 3 aromatic H of central ring), 8.13 (dd, 4 aromatic H ortho to  $\text{CO}_2\text{Ar}$ );  $^{13}\text{C-NMR}$  ( $\delta$  ppm TMS,  $\text{CDCl}_3$ ):  $\delta$  23.1, 28.3, 30.2, 68.1, 114.3, 115.8, 120.2, 123.5, 125.5, 127.1, 132.3, 139.6, 147.3, 148.6, 159.9, 160.5, 196.8; Anal. Calcd. for  $\text{C}_{32}\text{H}_{32}\text{O}_7$ : C, 72.70; H, 6.10; found: C, 72.69; H, 6.16.



### 3.3.6. Benzoic Acid, 4-(4-Pentenyl)-, 2-Methoxy-1,4-phenylene Ester (6)

4-(4-Pentenyl)benzoic acid (**1**, 1.04 g, 5.1 mmol), 2-methoxyhydroquinone (0.36 g, 2.56 mmol), DMAP (0.05 g, 0.4 mmol), and DCC (1.04 g, 5.1 mmol) in dry  $\text{CH}_2\text{Cl}_2$  (15 mL) were stirred at room temperature for 48 h. The product was extracted with water and methylene chloride. The precipitate of dicyclohexylurea by-product was filtered off and discarded. The solvent was removed using a rotary evaporator. The resulting solid was recrystallized from ethanol, resulting in 0.66 g (50%) of benzoic acid, 4-(4-pentenyl)-, 2-methoxy-1,4-phenylene ester (**6**) as white crystals.  $^1\text{H-NMR}$  ( $\delta$  ppm TMS,  $\text{CDCl}_3$ ): 1.95 (m,  $\text{CH}_2\text{CH}_2\text{O}$ , 4 H), 2.24 (m,  $\text{CH}_2\text{CH}=\text{CH}_2$ , 4 H), 3.80 (s,  $\text{OCH}_3$ ), 4.06 (t,  $\text{OCH}_2$ , 4 H), 5.05 (m,  $=\text{CH}_2$ , 4 H), 5.86 (m,  $=\text{CH}$ , 2 H), 6.89 (dd, 4 aromatic H ortho to OR), 7.19 (m, 3 aromatic H of central ring), 8.13 (dd, 4 aromatic H ortho to  $\text{CO}_2\text{Ar}$ );  $^{13}\text{C-NMR}$  ( $\delta$  ppm TMS,  $\text{CDCl}_3$ ):  $\delta$  28.2, 30.0, 56.0, 67.3, 106.6, 113.4, 114.1, 115.3, 121.2, 123.0, 132.2, 137.3, 149.0, 151.6, 163.2, 164.3. Anal. Calcd. for  $\text{C}_{31}\text{H}_{32}\text{O}_7$ : C, 72.03; H, 6.24; found: C, 72.20; H, 6.22.

### 3.3.7. Benzoic Acid, 4-(4-Pentenyl)-, 2-(Methyl)-1,4-phenylene Ester (7) [26]

4-(4-Pentenyl)benzoic acid (**1**, 1.12 g, 5.4 mmol), methylhydroquinone (0.7 g, 5.6 mmol), DMAP (0.07 g, 0.55 mmol), and DCC (1.5 g, 7.3 mmol) in dry  $\text{CH}_2\text{Cl}_2$  (15 mL) were stirred at room temperature for 48 h. The product was extracted with mixture of water and methylene chloride. The precipitate of dicyclohexylurea by-product was filtered off and discarded. The solvent was removed using a rotary evaporator. The resulting solid was recrystallized from mixture of ethanol (80%) and toluene (20%) to yield 1.8 g (65%) of benzoic acid, 4-(4-pentenyl)-, 2-(methyl)-1,4-phenylene ester (**7**) as white crystals.  $^1\text{H-NMR}$  ( $\delta$  ppm TMS,  $\text{CDCl}_3$ ): 1.86 (m,  $\text{CH}_2\text{CH}_2\text{O}$ , 4 H), 2.17 (s,  $-\text{CH}_3$ ), 2.21 (m,  $\text{CH}_2\text{CH}=\text{CH}_2$ , 4 H), 3.98 (t,  $\text{OCH}_2$ , 4 H), 4.98 (m,  $=\text{CH}_2$ , 4 H), 5.78 (m,  $=\text{CH}$ , 2 H), 6.89 (dd, 4 aromatic H ortho to OR), 7.03 (m, 3 aromatic H of central ring), 8.06 (dd, 4 aromatic H ortho to  $\text{CO}_2\text{Ar}$ );  $^{13}\text{C-NMR}$  ( $\delta$  ppm TMS,  $\text{CDCl}_3$ ):  $\delta$  16.9, 28.6, 30.4, 67.7, 114.5, 115.7, 120.3, 121.7, 123.1, 124.3, 132.3, 137.7, 147.2, 148.6, 163.6, 164.9.

## 4. Conclusions

A series of novel calamitic liquid crystalline compounds that exhibit a broad nematic liquid crystalline range was synthesized and characterized. These mesogens contain reactive double bonds on the termini of the aliphatic chains, functionality that may serve to incorporate these liquid crystalline moieties into a polymeric materials in future research (*e.g.*, formation of nematic elastomers). DSC investigations revealed the presence of liquid crystal phases by detecting the enthalpy change associated with the phase transition; the amount of energy released or absorbed can be used as a preliminary detection and identification of the liquid crystalline phase. Therefore, lower energy transitions are typically associated with the nematic phase; while, higher energy transitions are normally associated with smectic and crystalline phases. The identification of the mesophases was accomplished with variable temperature optical polarized light microscopy. Phase texture (morphology) observations and transitions were found to be consistent with the DSC results. Finally, the clearing points of the mesogens were greatly affected by the size of the lateral substituents, and

decreased with increasing lateral substituent size, making this class of liquid crystals particular promising as their thermotropic properties can be readily modulated by changes in the molecular structure.

### Acknowledgments

The authors wish to acknowledge support from the National Science Foundation (CHE-0832622).

### References

1. Demus, D.; Goodby, J.; Gray, G.W.; Spiess, H.W.; Vill, V. Low molecular weight liquid crystals. In *Handbook of Liquid Crystals*, 1st ed.; Demus, D., Ed.; Wiley-VCH: Weinheim, Germany, 1998; Vol. 2B, pp.15–18.
2. Collings, P.J.; Michael, H. *Introduction to Liquid Crystals*, 1st ed.; Taylor & Francis Ltd: London, UK, 1997; pp. 70–71.
3. Bahadur, B. *Liquid Crystals Application and Uses*, 1st ed.; World Scientific Publishing: Singapore, 1990; p. 11.
4. Collings, P.J.; Patel, J.S. *Handbook of Liquid Crystal Research*, 1st ed.; Taylor & Francis Ltd: London, UK, 1997; p. 600.
5. Jones, B. Apparent cases of liquid-crystal formation in p-alkoxybenzoic acids. *J. Chem. Soc.* **1935**, *1*, 1874.
6. Gray, G.W.; Jones, B. Mesomorphism and chemical constitution and the effect of halogen substitution on the mesomorphism of the 4-alkoxybenzoic acids. *J. Chem. Soc.* **1954**, *1*, 2556–2562.
7. Weissflog, W.; Moeckel, P.; Tschimeg, S.; Kresse, H.; Demus, D. Synthesis and dielectric properties of liquid crystalline alkyliminomethyl-substituted phenyl benzoates. *J. Prakt. Chem.* **1981**, *323*, 599–606.
8. Weissflog, W.; Demus, D.; Diele, S.; Nitschke, P.; Wedler, W. From laterally branched mesogens to novel twin molecules. *Liq. Cryst.* **1989**, *5*, 111–122.
9. Weissflog, W.; Demus, D. Thermotropic liquid-crystalline compounds with lateral long chain substituents, liquid-crystalline compounds with lateral aromatic branches. *Liq. Cryst.* **1988**, *3*, 275–284.
10. Baumeister, U.; Kosturkiewicz, Z.; Hartung, H.; Demus, D.; Weissflog, W. Thermotropic liquid-crystalline compounds with lateral long chain substituents, crystal and molecular structure of mesogenic 4-ethoxy-3'-(4-ethoxyphenyliminomethyl)-4'-(4-methoxybenzoyloxy) azobenzene. *Liq. Cryst.* **1990**, *7*, 241–249.
11. Ganicz, T.; Stanczyk, W.A.; Gladkova, N.K.; Sledzinska, I. Vinylsilanes as monomers for side chain polymer liquid crystals. *Macromolecules* **2000**, *33*, 289–293.
12. Yao, N.; Jamieson, A.M. Transient shear flow behavior of dilute solutions of side-chain liquid-Crystalline polysiloxanes in 4,4'-(n-pentyloxy) cyanobiphenyl. *Macromolecules* **1998**, *31*, 5399–5406.
13. Hsu, C.S.; Chu, P.H.; Chang, H.L.; Hsieh, T.H. Effect of lateral substituents on the mesomorphic properties of side-chain liquid crystalline polysiloxanes containing 4-[(S)-2-methyl-1-butoxy]

- phenyl 4-(alkenyloxy) benzoate side groups. *J. Polym. Sci. A, Polym. Chem.* **1997**, *35*, 2793–2800.
14. Inoue, A.; Maniwa, S.; Ide, V. Relation between molecular structure and electrorheological effects in liquid crystalline polymers. *J. Appl. Polym. Sci.* **1997**, *64*, 303–310.
  15. Jeng, G.P.C.; Kuo, J.F.; Chen, C.Y. X-ray investigation of terminally carboxyl oligo (ethylene oxide) monomethyl ethers-substituted side-chain liquid-crystalline polysiloxanes. *J. Appl. Polym. Sci.* **1993**, *47*, 781–788.
  16. Finkelmann, H.; Kock, H.J.; Rehage, G. Investigations on liquid crystalline polysiloxanes Liquid crystalline elastomers—A new type of liquid crystalline material. *Makro. Chem. Rap. Commun.* **1981**, *2*, 317–322.
  17. Kleinschmidt, F.; Hickl, M.; Saalwaechter, K.; Schmidt, C.; Finkelmann, H. Lamellar liquid single crystal hydrogels: Synthesis and investigation of anisotropic water diffusion and swelling. *Macromolecules* **2005**, *38*, 9772–9782.
  18. Weiss, F.; Finkelmann, H. Hexagonal lyotropic liquid crystalline hydrogels: Influence of uniaxial stress and pH value on the anisotropic swelling behavior. *Macromolecules* **2004**, *37*, 6587–6595.
  19. Amigo M.A.; Finkelmann, H. A concept for bifocal contact- or intraocular lenses: Liquid single crystal hydrogels. *Polym. Adv. Technol.* **2002**, *13*, 363–369.
  20. Petri, A.; Braeuchle, C.; Leigeber, H.; Miller, A.; Weitzel, H.P.; Kreuzer, F.H. Cholesteric liquid crystalline siloxanes with azo dye: Generation of additional reflection bands with linearly polarized light. *Liq. Cryst.* **1993**, *15*, 113–121.
  21. Loth, H.; Foltin, U. Methoxy-polyethoxy side-chain silastomers as materials controlling drug delivery by diffusion flux. *Controlled Release* **1998**, *54*, 273–282.
  22. Sio, Li.; Veltri, A.; Umetron, C.; Serak, S; Tabiryan, N. All-optical switching of holographic grating made of polymer-liquid-crystal slices containing azo-compounds. *Appl. Phys. Lett.* **2008**, *18*, 151–153.
  23. Percec, V.; Chu, P. Molecular and supramolecular liquid crystalline dendrimers. *Polym. Mater. Sci. Eng.* **1995**, *73*, 125–126.
  24. Percec, V.; Kawasumi, M. Synthesis and characterization of thermotropic liquid-crystalline dendrimers. *Polym. Prepr. (Am. Chem. Soc., Div. Polym. Chem.)* **1993**, *34*, 158–159.
  25. Percec, V.; Wang, C.S. Synthesis and characterization of polymethacrylates, polyacrylates, and poly(methylsiloxane)s containing 4-[S(-)-2-methyl-1-butoxy]-4'-(w-alkanyl-1-oxy)-alpha -methylstilbene side groups. *J. Macromol. Sci., Part A: Pure. Appl. Chem.* **1992**, *2*, 99–121.
  26. Arehart, S.V.; Pugh, C. Induction of smectic layering in nematic liquid crystals using immiscible components. Laterally attached side-chain liquid crystalline poly norbornenes and their low molar mass analogs with hydrocarbon/fluorocarbon substituents. *J. Am. Chem. Soc.* **1997**, *119*, 3027–3037.
  27. Kumar, U.; Kato, T.; Frechet, J. Use of intermolecular hydrogen bonding for the induction of liquid crystallinity in the side chain of polysiloxane. *J. Am. Chem. Soc.* **1992**, *114*, 6630–6639.